Determination of Lipid Phase Transition Temperatures in Hybrid Bilayer Membranes

Neil A. Anderson, Lee J. Richter, John C. Stephenson, and Kimberly A. Briggman*

The National Institute of Standards and Technology, 100 Bureau Drive MS8443, Gaithersburg, Maryland 20899

Received June 23, 2006

The main gel-to-liquid-crystal (LC) phase transition temperature, T_m, of the lipid monolayer in hybrid bilayer membranes (HBMs) was investigated using vibrational sum frequency spectroscopy (VSFS). In the gel phase, the acyl chains of the lipid molecules assume an ordered, all-trans configuration, whereas in the LC phase, the acyl chains exhibit a significant number of disordered gauche conformers. VSFS has unique sensitivity to the order/disorder transitions in the acyl chains and was used to determine T_m for a series of saturated phosphatidylcholine lipids on octadecanethiolate self-assembled monolayers (SAMs). The values obtained for T_m for all lipids studied are significantly higher than for the corresponding lipids in vesicles in solution. Additionally, the transition widths are broader for the lipids in HBMs. The underlying SAM clearly influences the phase behavior of the overlying lipid monolayer.

Introduction

Supported planar bilayers (SPBs) have provided a convenient platform for interrogating membrane properties and function.[1] To overcome the inherent fragility of SPBs, hybrid bilayer membranes (HBMs) have been developed.[2] HBMs, composed of an alkanethiolate self-assembled monolayer (SAM) covalently linked to a gold surface with a phospholipid monolayer overlayer, offer increased membrane-substrate stabilization over traditional SPBs. Although their use as model biosensors has already been demonstrated,[3] HBMs are also being explored as cell membrane mimics. In natural cell membranes, the dynamic and fluidic properties of the lipid membrane are crucial to their biological activity. Therefore, for HBMs to be broadly applicable as biosensors or biomimetic platforms, it is critical to determine the fluidity of the lipid layer. In this study, we report measurements of the main thermal phase transition temperature, T_m, for a series of saturated phosphatidylcholine lipid monolayers on octadecanethiolate (ODT) SAMs. The results demonstrate that the ODT SAM significantly influences the lipid layer. The phase transition temperature of the lipid layer increases by about 10 °C and the transition width significantly broadens relative to the corresponding lipids in vesicles or multilamellar bilayers. The implications on both our fundamental understanding of phase transitions in lipid layers and on the technological applications of HBMs are discussed.

Although there have been no previous studies of the thermal phase transitions involving lipid/alkanethiolate HBMs, there is vast literature on the phase transitions of lipids in vesicles or in hydrated multilamellar lipid bilayers. These have been studied through differential scanning calorimetry (DSC),[4] nuclear magnetic resonance (^{1}H NMR),[5] X-ray[6] and neutron[7] scattering, Raman[8,9] and infrared (IR)[9,10] vibrational spectroscopies, fluorescence microscopy[11] of dyes inserted in the lipid layers, and scanning probe microscopy (SPM).[12] Except for SPM, most of these techniques lack the sensitivity to study a single supported monolayer. There have also been extensive analytical modeling and molecular dynamics (MD) simulations[13] performed for lipid bilayers. In this study, we use the interface sensitive nonlinear optical technique of vibrational sum frequency spectroscopy (VSFS) to monitor the main thermal gel to liquid crystalline (LC) phase transition for the lipid monolayer in HBMs. VSFS offers submonolayer sensitivity and the usual strengths of vibrational specificity shared by Raman scattering and IR absorption spectroscopies. It is particularly sensitive to molecular orientation. Additionally, because VSFS is symmetry forbidden in systems that are locally centrosymmetric, it is well suited to the order/disorder changes that characterize melting of lipidic acyl chains. It is now well accepted that vibrational transitions associated with the presence of gauche conformers in lipidic acyl chains reflect the degree of disorder of chains in both linear[9] and nonlinear spectroscopies.[14,15] Our experimental implementation of broadband VSFS is particularly well suited to biological material studies and has been previously described in detail.[16]

Experimental Section

Certain equipment, instruments, or materials are identified in this paper in order to adequately specify the experimental details. Such identification does not imply recommendation by the National

* To whom correspondence should be addressed. E-mail: kimberly.briggman@nist.gov.

(1) Richter, R. P.; Him, J. L. K.; Brisson, A. *Mater. Today* **2003**, *6*, 32−37.
(2) Plant, A. *Langmuir* **1999**, *15*, 5128−5135.
(3) Cornell, B. A.; Braach-Maksvytis, V. L. B.; King, L. G.; Osman, P. D. J., Raguse, B.; Wieczorek, L.; Rice, R. J. *Nature* **1997**, 387, 580−583.
(4) Lewis, R..; Mak, N.; McElhaney, R. N. *Biochemistry* **1987**, *26*, 6118−6126.
(5) Kennedy, A.; Hmel, P. J.; Seelbaugh, J.; Quiles, J. G.; Hicks, R.; Reid, T. J. *J. Liposome Res.* **2002**, *12*, 221−237.
(6) Caffrey, M.; Wang, J. *Annu. Rev. Biophys. Biomol. Struct.* **1995**, *24*, 351−378.
(7) Pabst, G.; Katsaras, J.; Raghunathan, V. A.; Rappolt, M. *Langmuir* **2003**, *19*, 1716−1722.
(8) Pink, D. A.; Green, R. J.; Chapman, D. *Biochemistry* **1980**, *19*, 349−356.
(9) Levin, I. W. In *Advances in Infrared and Raman Spectroscopy*; Clark, R. J. H., Hester, R. E., Eds.; Heyden-Wiley: Chichester, U.K., 1984; Vol. 11, p 1.
(10) Mantsch, H. H.; McElhaney, R. N. *Chem. Phys. Lipids* **1991**, *57*, 213−226.
(11) Shinitzky, M.; Barenholz, Y. *Biochim. Biophys. Acta* **1978**, *515*, 367−394.
(12) Giocondi, M.-C.; Grimellec, C. L. *Biophys. J.* **2004**, *86*, 2218−2230.
(13) Pastor, R. W.; Venable, R. M.; Feller, S. E. *Acc. Chem. Res.* **2002**, *35*, 438−446
(14) Guyot-Sionnest, P.; Hunt, J. H.; Shen, Y. R. *Phys. Rev. Lett.* **1987**, *59*, 1597−1600.
(15) Gurau, M. C.; Castellana, E. T.; Albertorio, F.; Kataoka, S.; Lim, S.-M.; Yang, R. D.; Cremer, P. S. *J. Am. Chem. Soc.* **2003**, *125*, 11166−11167.
(16) Richter, L. J.; Petralli-Mallow, T. P.; Stephenson, J. C. *Opt. Lett.* **1998**, *23*, 1594−1596.

10.1021/la061819e
Published on Web 09/02/2006

Institute of Standards and Technology nor does it imply the materials are necessarily the best available for the purpose.

Vibrational Sum Frequency Spectroscopy. VSFS spectra were acquired using a nominally 50 fs Ti-sapphire laser to produce broad bandwidth IR pulses that were mixed with a narrowed (6 cm^{-1}) bandwidth 810 nm pulse from a ps Ti-sapphire amplifier. These beams were brought into coincidence in time and space at the gold sample surface. Typical pulse energies, beam diameters, and incident angles from the surface normal were 3.5 μJ, 200 μm, and 67° (dry) for the IR beam, and 10 μJ, 400 μm, and 45° (dry) for the 810 nm beam, respectively. All VSFS spectra shown were acquired in the *ppp* polarization combination. The VSFS generated light is collected and dispersed in a spectrometer and detected with a liquid-nitrogen-cooled CCD array similar to that reported previously.[17] The VSFS spectra were fit to the following equation:

$$I_{\mathrm{VSFS}}(\omega_{\mathrm{IR}}) \propto \left|B + \sum_q \frac{A_q e^{i\phi_q}}{\omega_{\mathrm{IR}} - \omega_q + i\Gamma_q}\right|^2 \qquad (1)$$

The first term, *B*, arises from the nonresonant contribution to the nonlinear susceptibility, $\chi^{(2)}$, due to the gold substrate. The second term reflects a sum of the resonant contributions to $\chi^{(2)}$ from each vibrationally active mode, *q*, of molecules at the interface. Lorentzian line shapes adequately described the data. Each mode has amplitude, A_q, center frequency, ω_q, line width, Γ_q, and phase component, ϕ_q.[18] The VSFS data for the acyl lipid chains were fit to seven peaks determined from a previous study of a closely related system, alkanethiolate SAMs on Au.[19] The fit frequencies and assignments for the C−H vibrational modes are CH_2 symmetric stretch (d^+) at 2845 cm^{-1}, CH_2 symmetric stretch of the terminal methylene adjacent to the CH_3 (d_t^+) at 2860 cm^{-1}, CH_3 symmetric stretch (r^+) at 2873 cm^{-1}, CH_2 asymmetric stretch (d^-) at 2898 cm^{-1}, CH_3 Fermi resonance (r^+_{FR}) at 2935 cm^{-1}, CH_3 out-of-plane asymmetric stretch (r^-_{op}) at 2959 cm^{-1}, and CH_3 in-plane asymmetric stretch (r^-_{ip}) at 2978 cm^{-1}. The C−H stretches related to the choline CH_3 are not pronounced in any of our studies. Recently, the frequencies of these modes were reported to be at 2975 and 3053 cm^{-1} for the choline CH_3 symmetric and asymmetric stretches, respectively.[20] Since we are using only the lowest frequency modes <2875 cm^{-1} to determine T_m, even if the choline modes were present, it would not change any conclusions of this study. For facile comparison of mode amplitudes, the widths of the d^+, d_t^+, and r^+ modes were held constant at 7, 6, and 6 cm^{-1}, respectively, and the frequencies of the fitted peaks were constrained to vary only ±3 cm^{-1} from the listed peak values. The ratios of the amplitudes of the d^+/r^+ modes were used for analysis of the degree of order/disorder of the lipid chains. It is has been shown before that vibrational transitions associated with the lipidic acyl chains reflect the order/disorder of chains in VSFS.[15]

Chemicals and Materials. 1,2-Dimyristoyl-*sn*-glycero-3-phosphocholine, DMPC, 1,2-dipentadecanoyl-*sn*-glycero-3-phosphocholine, D(C_{15})PC, and 1,2-dipalmitoyl-*sn*-glycero-3-phosphocholine, DPPC, were obtained from Avanti Polar Lipids (Alabaster, AL) as lyophilized powders (>99%). Histological grade 2-propanol was purchased from Sigma Aldrich Co. (St. Louis, MO) and dried with molecular sieves before use. Deuterium oxide, D_2O, (99.9%) was obtained from Cambridge Isotope Laboratories, Inc. (Andover, MA). Perdeuterated phosphate buffered saline, dPBS, solutions were prepared by adding packets of dried PBS (0.1 M phosphate buffered saline; 0.138 M sodium chloride; 0.0027 M potassium chloride; pH 7.4) obtained from Sigma Aldrich Co. (St. Louis, MO) to D_2O. Perdeuterated octadecanethiol (dODT) was custom synthesized by Prochimia Surfaces Sp. z o.o. (Poland). 200-proof ethanol was used as received from Warner Graham, Inc. (Cockeysville, MD). Titanium and gold coated slides were custom coated by Platypus Technologies, LLC (Madison, WI).

HBM Preparation. The HBM samples were formed on gold coated glass microaqueduct slides (custom fabricated, bare glass slides were obtained from Bioptechs Inc. (Butler, PA)). The gold slides have 5 nm Ti as the adhesion layer and a 250 nm film of gold. The gold surface was cleaned by UV ozone, rinsed with ultrapure, deionized water, and recleaned with UV ozone. The cleaned gold surface was immediately immersed in a 200 μM ethanolic solution of dODT for at least 14 h. It was then rinsed with ethanol and ultrapure deionized water and dried in a stream of pure, dry N_2 gas. SAM formation was verified by infrared reflection-adsorption spectroscopy (IRAS), vibrational sum-frequency spectroscopy (VSFS), and ellipsometry. The slide with the SAM was then mounted in a brass variable temperature cell. A 15 μm Teflon spacer separated the SAM slide from the top 2 mm thick CaF_2 window through which the incident IR and visible beams passed. The gold coated, SAM covered slide is made with two pairs of parallel grooves roughly 10 mm long that allow laminar flow in two isolated 20 mm long channels across the sample. A peristaltic pump was used to push solution through the cell at a flow rate of about 1 mL·min^{-1}. The top lipid layer of the HBM was deposited by flowing lipid vesicles in through the 15 μm space between the CaF_2 window and the SAM in one of the channels, whereas only perdeuterated aqueous solution was present in the other channel. This latter channel provided a reference VSFS spectrum for the HBM in the former channel.

The vesicles were formed by the injection method:[21] 1.5 mg (2 μmol) of phospholipids was weighed out, dissolved in 20 μL dry 2-propanol and injected with a pipet tip into 1 mL of vortexing D_2O or dPBS. The solution was diluted by 10 to produce a 200 μM concentration before use. As reported previously, the liposomes spontaneously unfold (fuse) on the SAM, forming the lipid overlayer of the HBM, as previously verified through VSFS.[22] After the HBM was formed, pure D_2O or deuterated buffer was flowed through the cell; all VSFS spectra were acquired with D_2O or deuterated buffer flowing over the HBM. For phase transition studies, the temperature of the brass cell was controlled by flowing water from a thermostated water source through the brass cell. The cell was allowed to stabilize for 5 min at each temperature before data acquisition began. The temperature was measured with a calibrated chromel−alumel thermocouple with a precision of ±0.1 °C and absolute accuracy of ±0.5 °C in contact with the back of the glass microaqueduct slide.

Results and Discussion

HBMs consisting of a phosphatidylcholine (PC) lipid monolayer on an ODT SAM have been extensively studied. In this study, a series of saturated PC lipids: DMPC, D(C_{15})PC, and DPPC was used for determination of T_m for HBMs. For spectral simplicity, we used a fully perdeuterated analogue of ODT ($CD_3(CD_2)_{17}SH$ or dODT) for the SAM and fully protonated lipids. Figure 1 shows the VSFS spectra in the C−H stretching region for an HBM composed of a DPPC layer over a dODT SAM as a function of temperature, *T*, in contact with perdeuterated aqueous solution. For $T < T_m$ (~50 °C), DPPC is in its gel phase in which the methylene groups in the lipidic acyl chains assume a nearly all-trans configuration, whereas for $T > T_m$, the lipids are in the LC phase in which the acyl chains exhibit a significant number of gauche conformers. All-trans conformers result in near cancellation of the VSFS signal from the ordered alternating methylene (CH_2) groups. Therefore, the spectra below T_m are dominated by the three strong features associated with the ordered, terminal CH_3 group. However, the introduction of

(17) Yang, C. S. C.; Richter, L. J.; Stephenson, J. C.; Briggman, K. A. *Langmuir* **2002**, *18*, 7549−7556.

(18) The amplitude A_q reflects the intrinsic resonant susceptibility $\chi_R^{(2)}$, Frensel factors and local field corrections. As each mode has a distinct $\chi_R^{(2)}$, and the VSFS *ppp* polarization combination probes all 4 unique symmetry allowed (for $C_{\infty v}$) elements of $\chi_R^{(2)}$, ϕ_q will generally be distinct for each mode *q*.

(19) Himmelhaus, M.; Eisert, F.; Buck, M.; Grunze, M. *J. Phys. Chem. B* **2000**, *104*, 576−584.

(20) Liu, J.; Conboy, J. C. *Langmuir* **2005**, *21*, 9091−9097.

(21) Silin, V. I.; Wieder, H.; Woodward, J. T.; Valincius, G.; Offenhausser, A.; Plant, A. L. *J. Am. Chem. Soc.* **2002**, *124*, 14676−14683.

(22) Petralli-Mallow, T.; Briggman, K. A.; Richter, L. J.; Stephenson, J. C.; Plant, A. L. *Proc. SPIE−Int. Soc. Opt. Eng.* **1999**, *3858*, 25−31.

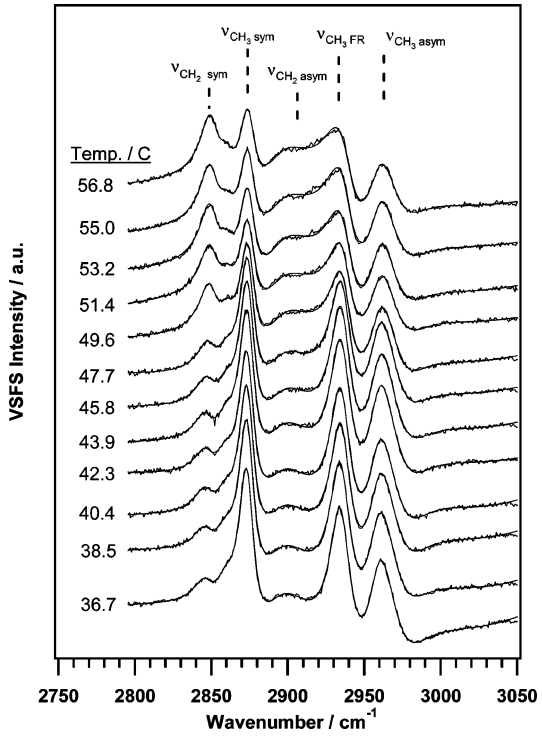

Figure 1. VSFS spectra of a DPPC/dODT HBM in contact with aqueous solution as a function of temperature. The VSFS spectra are taken with *ppp* polarization and are offset for clarity. Solid lines drawn through the spectra are quantitative fits to the data.

gauche conformers breaks the centrosymmetry of the acyl chains and allows CH_2 modes to appear in the spectra. This is concomitant with a loss of intensity of the CH_3 modes as the acyl chains become more disordered. At $T > T_m$, the spectra develop prominent CH_2 vibrational modes, that become of comparable magnitude to the CH_3 modes. The lines through the data in Figure 1 are the result of quantitative fits to eq 1 to determine amplitudes of the individual vibrational modes.

The ratio of the amplitude of the CH_2 d^+, A_{CH2}, at 2845 cm^{-1} to that of the CH_3 r^+, A_{CH3}, at 2873 cm^{-1} is a quantitative measure of the disorder in acyl chains.[15] This ratio derived from the data presented in Figure 1, is shown in Figure 2c (solid squares). At T_m, the A_{CH2}/A_{CH3} ratio increases suddenly. Previously, spectroscopic changes with T near T_m of the lipid multilayers have been fit to a sigmoid function:[23] $S(T) = C + A/(1 + \exp((T - T_m)/D))$, where C is a constant, A is the amplitude, T is the temperature, T_m is the midpoint of the phase transition, and D is a width factor related to the enthalpy of transition and to the effective domain size. Shown in Figure 2 are the least-squares fits (lines) to this form used to determine the phase transition temperature, T_m, for each HBM system. The transition widths have been determined from the full width at half-maximum (fwhm) of the derivative of the sigmoid fit.[5] Fitting the A_{CH2}/A_{CH3} ratio from Figure 1 gives $T_m = 49.4$ °C ± 0.2 °C[24] for DPPC on dODT. For comparison and as a check on variability, also shown in Figure 2c is a data set for another prepared DPPC/dODT HBM (open squares). T_m obtained from the second data set is 51.4 °C ± 0.4 °C.[24] These values of T_m are ~9 °C greater than the value $T_m = 41.4$ °C reported for DPPC vesicles[25]

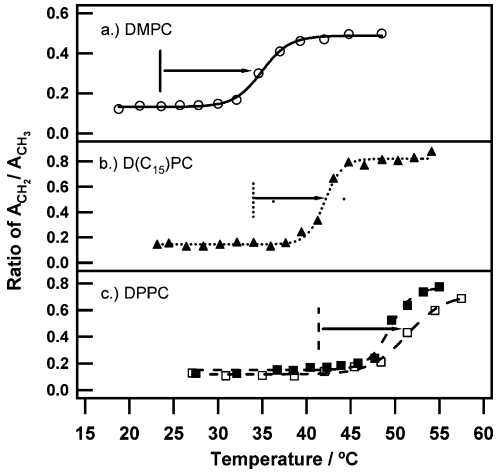

Figure 2. Ratios of A_{CH2}/A_{CH3} for (a) DMPC/dODT, (b) D(C_{15})-PC/dODT, and (c) DPPC/dODT HBMs as a function of temperature. The lines through the data are the result of fitting to a sigmoid function. The vertical lines represent T_m for corresponding vesicles in solution.

Table 1. Transition Temperature and Widths Observed for Lipids in dODT-Based HBMs

lipid	T_m (°C) for vesicles	T_m (°C) for HBM	transition width (°C)
DMPC	23.5[25]	35.0 ± 0.2[24]	5.5
D(C_{15})PC	34.0[25]	42.1 ± 0.1[24]	3.5
DPPC (■)	41.4[25]	49.4 ± 0.2[24]	4.5
DPPC (□)	41.4[25]	51.4 ± 0.4[24]	7.4

(represented by a vertical line). Also shown in Figure 2a,b are the A_{CH2}/A_{CH3} ratios for HBMs of DMPC/dODT and of D(C_{15})-PC/dODT and their sigmoid fits, respectively. The determined values of T_m and the transition widths are summarized in Table 1. Note that for all three HBMs the T_m for the lipid layer is about 10 °C higher than reported for the respective lipid in a vesicle. VSFS spectra of the underlying dODT SAM (data not shown) establish that it remains intact and crystalline at all temperatures below 60 °C.

Although this is the first T_m data for HBM lipid layers, a variety of methods have assessed T_m for related SPBs. An analysis of the reported T_m for various SPBs allows their grouping into the following categories: lipid bilayers on glass or silica, lipid bilayers on mica, and lipid monolayers on hydrophobic, silanized surfaces. The T_m for PC lipid bilayers fused to planar glass substrates have been investigated by VSFS[26] and TIR Raman.[27] PC bilayers have also been assembled on silica beads[28] (which provide increased surface area and curvature). These papers report little interaction between the glass substrate and the supported PC bilayers and T_m is reported to be at nearly the same temperature as unsupported PCs in vesicles.

T_m has been measured for PC bilayers supported on mica substrates. DSC experiments for DPPC and D(C_{15})PC multilayers on high surface area mica chips[29] revealed several phase transitions: one at T_m similar to vesicles and two more at T_m + 2 °C and T_m + 4 °C higher than vesicles. The lowest T_m was attributed to the multilayer, the next higher T_m to the top leaflet of the mica-bound bilayer, and the highest T_m to the lower leaflet closest to the mica. This result was more recently confirmed for

(23) Kirchoff, W. H.; Levin, I. W. *J. Res. Natl. Bur. Stand.* **1987**, *92*, 113−128.
(24) Uncertainties are one standard deviation based on the diagonal elements of the error matrix.
(25) Marsh, D. *CRC Handbook of Lipid Bilayers*; CRC Press: Boca Raton, FL, 1990; pp 136 and 153.
(26) Liu, J.; Conboy, J. C. *J. Am. Chem. Soc.* **2004**, *126*, 8894−8895.
(27) Lee, C.; Bain, C. D. *Biochim. Biophys. Acta* **2005**, *1711*, 59−71.
(28) Naumann, C.; Brumm, T.; Bayerl, T. M. *Biophys. J.* **1992**, *63*, 1314−1319.
(29) Yang, J.; Appleyard, J. *J. Phys. Chem. B* **2000**, *104*, 8097−8100.

bilayers on mica with AFM.[30] It was proposed that an electrostatic interaction between the headgroup of the lower lipid leaflet with the mica surface increases T_m for that layer, and also propagates weakly to an increase in T_m for the second layer (top leaflet of the mica-bound layer).

T_m has been determined by DSC and ^{2}H NMR for d_{62}-DPPC monolayers on C18 silanized spherical glass beads[31] and is reported to be 8.6 °C higher than d_{62}-DPPC multilamellar vesicles. However, in a subsequent publication involving HBMs of protonated lipids on similarly silanized silica,[32] a trend in T_m for PC lipids ranging from 1,2-dilauroyl-*sn*-glycero-3-phosphocholine, DLPC (C12), to 1,2-diarachidoyl-*sn*-glycero-3-phosphocholine, DAPC (C20), is observed. For HBMs on C18-silanized silica, T_m is reported to be 18.1 °C higher for DLPC, 11.2 °C higher for DMPC, 5.6 °C higher for DPPC, 1.3 °C *lower* for 1,2-distearoyl-*sn*-glycero-3-phosphocholine, DSPC (C18), and 8.6 °C *lower* for DAPC relative to T_m for the respective lipids in vesicles in solution. This trend is attributed by the authors to an interdigitized packing of the lipids into the hydrophobic silane layer with optimized packing for equal chain lengths, i.e., for DSPC (C18) in C18-silanized chains. Interdigitization may be possible for silanized layers on silica due to the decreased ordering of the C18-silane chains on silica,[33] which has been shown to depend on the pretreatment of the silica surface with hydroxyl or water moieties.

It is clear that the dominant physical interactions in the lipid/dODT HBMs presented here are different than proposed for either SPBs on mica or lipid monolayers on silanized silica. Since electrically neutral SAMs on uncharged Au are used, we can eliminate the possibility of electrostatic attraction of the lipid to the SAM covered Au surface. We can also eliminate simple interdigitation of the lipid layer into the dODT because of the high packing density of dODT molecules in the SAM which keeps the SAM crystalline and impenetrable at all temperatures investigated in this study ($<$60 °C), consistent with previous studies of the melting temperature of related alkanethiolate systems.[34,35,36] Moreover, preliminary data in our lab for DSPC/dODT HBMs indicates that T_m is significantly higher than the 55.1 °C[25] observed for DSPC vesicles, and recent VSFS data for HBMs of a related lipid 1,2-distearoyl-*sn*-glycero-3-[phospho-rac-(1-glycerol)], DSPG, on dODT[37] at 60 °C (T_m for DSPG vesicles is 54.5 °C[25]) that indicate the lipid is clearly in the ordered gel phase. Thus, the mechanism for the increased T_m in our lipid/dODT HBMs is different than mechanisms proposed for related SPBs.

The systems studied here exhibit transition widths from the sigmoid fits that range from 3.5 to 7.4 °C. These widths are much greater than the typical $\leq$1 °C widths reported by DSC thermograms or IR frequency shifts for large unilamellar or multilamellar vesicles.[5] The broader transition widths observed here may be related to a decrease in cooperativity between the lipid molecules in the monolayer or due to the small cooperative unit sizes observed for related systems.[38]

Although it is not within the scope of this paper to provide a quantitative model for the results presented here, we offer possible explanations for both the increased and broadened T_m for alkanthiolate HBMs. Perhaps the interaction of the hydrophobic lipid tails with the dODT surface effectively confines the lipids inhibiting the lateral expansion of the lipid layer, which is known to take place at T_m, thus raising T_m in HBMs relative to SPBs. Lipid confinement could lead to a smaller cooperative unit size undergoing the melting transition, which would broaden the transition width. Alternatively, the inability of lipids to interdigitate into dODT, as evidenced by the crystallinity of dODT at all temperatures in this study and by the lack of a pretransition ripple phase, could also contribute to increasing T_m. Although we can offer no definitive model to explain our results, we expect this to be a general effect of the interaction of a nearly perfect, crystalline organic substrate with a lipid layer.

As alkanethiolate HBMs continue to be used to support membrane-associated proteins[37,39] and to be developed as electrical biosensors, implications of a raised T_m of the lipid layer in HBMs are increasingly important to acknowledge. For example, it has been shown in vesicles that a fluid bilayer is needed to allow protein diffusion for efficient enzyme catalytic activity: a 4-fold increase in activity was observed between cytochrome and cytochrome b5 reductase upon raising the temperature to the vesicle phase transition temperature.[40] If HBMs are to be used to mimic vesicle bilayers systems, the phase state of the lipid layers must be known and controlled.

Conclusions

For the HBM systems presented in this paper, a lipid PC monolayer is in contact with an immobilized, crystalline SAM. For a series of saturated PC lipids, the SAM stabilizes the gel phase of the lipid layer for ~10 °C above the usual lipid vesicle T_m. Possible reasons for the increase in T_m include inhibition of the expansion of the lipid layer (which necessarily occurs upon melting) by interaction with the dODT layer, and the inability of lipids to interdigitate into the crystalline dODT. We also observe a broader phase transition temperature width for the HBMs, ranging from 4 to 7 °C. These widths are much greater than the typical $\leq$1 °C widths reported by DSC thermograms or IR frequency shifts for large unilamellar or multilamellar vesicles.[5] The broader transition width observed here may be related to a decrease in cooperativity between the lipid molecules in the monolayer or due to the small cooperative unit sizes observed for related systems.[38] These observations establish that the phase state of the lipid cannot be taken from vesicle data when considering the use of HBMs as biological membrane mimics.

Acknowledgment. We gratefully acknowledge support from the NIST intramural Advanced Technology Program. N.A.A. acknowledges the National Research Council for postdoctoral fellowship support.

LA061819E

(30) Feng, Z. V.; Spurlin, T. A.; Gewirth, A. A. *Biophys. J.* **2005**, *88*, 2154−2164.
(31) Linseisen, F. M.; Hetzer, M.; Brumm, T.; Bayerl, T. M. *Biophys. J.* **1997**, *72*, 1659−1667.
(32) Käsbauer, M.; Bayerl, T. M. *Langmuir* **1999**, *15*, 2431−2434.
(33) Wang, R.; Guo, J.; Baran, G.; Wunder, S. L. *Langmuir* **2000**, *16*, 568−576.
(34) Schreiber, F.; Eberhardt, A.; Leung, T. Y. B.; Schwartz, P.; Wetterer, S. M.; Lavrich, D. J., Berman, L.; Fenter, P.; Eisenberger, P.; Scoles, G. *Phys. Rev. B* **1998**, *57*, 12476−12481.
(35) Bansebaa, F.; Ellis, T. H.; Badia, A.; Lennox, R. B. *J. Vacuum Sci. Technol. A* **1995**, *13*, 1331−1336.
(36) Schreiber, F.; Gerstenberg, M. C.; Dosch, H.; Scoles, G. *Langmuir* **2003**, *19*, 10004−10006.
(37) Doyle, A. W.; Fick, J.; Himmelhaus, M.; Eck, W.; Graziani, I.; Prudovsky, I.; Grunze, M.; Maciag, T.; Neivandt, D. J. *Langmuir* **2004**, *20*, 8961−8965.
(38) Tokumasu, F.; Jin, A. J.; Dvorak, J. A. *J. Electron Microsc.* **2002**, *51*, 1−9.
(39) Smith, M. B.; Tong, J.; Genzer, J.; Fischer, D.; Kilpatrick, P. K. *Langmuir* **2006**, *22*, 1919−1927.
(40) Strittmatter, P.; Rogers, M. J. *Proc. Natl. Acad. Sci. U.S.A.* **1975**, *72*, 2658−2661.